

1 **A new role for capsid assembly modulators to target mature hepatitis B virus**
2 **capsids and prevent virus infection**

3

4 Chunkyu Ko^a, Romina Bester^a, Xue Zhou^b, Zhiheng Xu^b, Christoph Blossey^a, Julia
5 Sacherl^a, Florian W. R. Vondran^{c,d}, Lu Gao^b, and Ulrike Protzer^{a,e#}

6

7 ^aInstitute of Virology, Technical University of Munich / Helmholtz Zentrum München,
8 Munich, Germany

9 ^bRoche Innovation Center Shanghai, Shanghai, China

10 ^cReMediES, Department of General, Visceral and Transplant Surgery, Hannover
11 Medical School, Hannover, Germany

12 ^dGerman Centre for Infection Research (DZIF), partner site Hannover-Braunschweig,
13 Hannover, Germany

14 ^eGerman Center for Infection Research (DZIF), Munich partner site, Munich,
15 Germany

16

17 Running title: HBV capsid modulators prevent infection

18

19 #Address correspondence to Ulrike Protzer, protzer@tum.de; [protzer@helmholtz-
muenchen.de](mailto:protzer@helmholtz-
20 muenchen.de); Institute of Virology, Technical University of Munich / Helmholtz
21 Zentrum München, Trogerstrasse 30, 81675 Munich, Germany; Tel: +49 8941406886;

22 Fax: +49 8941406823

23 **Abstract**

24 Hepatitis B virus (HBV) is a major human pathogen killing an estimated 887,000
25 humans per year. Therefore, potentially curative therapies are of high need.
26 Following infection, HBV deposits a covalently closed circular (ccc) DNA in the
27 nucleus of infected cells that serves as transcription template and is not affected by
28 current therapies. HBV core protein allosteric modulators (CpAMs) prevent correct
29 capsid assembly but may also affect early stages of HBV infection. In this study, we
30 aimed to determine the antiviral efficacy of a novel, structurally distinct
31 heteroaryldihydropyrimidine (HAP)-type CpAM, HAP_R01, and investigated whether
32 and how HAP_R01 prevents the establishment of HBV infection. HAP_R01 shows a
33 significant inhibition of cccDNA formation when applied during the first 48 h of HBV
34 infection. Inhibiting cccDNA formation, however, requires $>1 \log_{10}$ higher
35 concentrations than inhibition of the assembly of newly forming capsids (half-
36 maximal effective concentration (EC_{50}) 345-918 nM versus 26.8-43.5 nM,
37 respectively). Biophysical studies using a new method to detect the incoming capsid
38 in *de novo* infection revealed that HAP_R01 can physically change mature capsids
39 of incoming virus particles and affect particle integrity. Treating purified HBV virions
40 with HAP_R01 reduced their infectivity, highlighting the unique antiviral activity of
41 CpAMs to target the capsid within mature HBV particles. Accordingly, HAP_R01
42 shows an additive antiviral effect in limiting *de novo* infection when combined with
43 viral entry inhibitors. In summary, HAP_R01 perturbs capsid integrity of incoming
44 virus particle, reduces their infectivity and thus inhibits cccDNA formation in addition
45 to preventing HBV capsid assembly.

46 Introduction

47 Hepatitis B virus (HBV) infection is a global health problem with 257 million chronic
48 carriers worldwide who are at a high risk of developing liver diseases such as liver
49 cirrhosis and hepatocellular carcinoma (1). Although new infections and mother-to-
50 child transmission can be controlled by hepatitis B vaccine, hepatitis B
51 immunoglobulin (HBIG) and potent antivirals, hepatitis B surface antigen (HBsAg)
52 seroprevalence is estimated over 8% in high endemic areas, especially in Sub-
53 Saharan Africa and in Asia (2). Curative treatment options for individuals already
54 infected with HBV are still lacking. Current treatment of chronic hepatitis B includes
55 orally administered nucleos(t)ide analogues (NUCs), such as entecavir (ETV) and
56 tenofovir (TDF) that inhibit the reverse transcriptase activity of HBV polymerase, and
57 subcutaneously administered interferons. NUCs efficiently suppress virus replication,
58 have an excellent safety profiles and can reduce the risk of liver-disease and
59 mortality. However, NUCs cannot eliminate episomal covalently closed circular (ccc)
60 DNA that serves as the template for viral transcription and represents the viral
61 persistence form (3). Thus, there is a high need to develop new and potentially
62 curative therapeutic approaches that target cccDNA.

63 HBV is a small enveloped virus containing partially double-stranded, relaxed circular
64 (rc) DNA within its capsid (4). The icosahedral HBV capsid spontaneously assembles
65 from 120 dimers of HBV core protein. HBV core protein and its assembled capsid
66 play a role in virtually every step of HBV life cycle. During cell entry, the incoming
67 particle releases the capsid that delivers the HBV rcDNA genome into the nucleus
68 where rcDNA is converted into cccDNA. Core protein associates with cccDNA and is
69 implicated in epigenetic regulation of cccDNA (5). Later in infection, viral DNA
70 synthesis occurs within newly-assembled capsids via reverse transcription of a

71 pregenomic RNA (pgRNA) giving rise to rcDNA. During formation of new viral
72 genomes, capsids facilitate pgRNA packaging, minus-strand and plus-strand DNA
73 synthesis rather than being inert containers (6-8). Subsequently, rcDNA-containing
74 capsids are enveloped and released from the cells or alternatively recycled back to
75 the nucleus to maintain or amplify cccDNA (9).

76 Core protein allosteric modulators (CpAMs), also called capsid assembly inhibitors,
77 are small molecules capable of modulating capsid assembly (10). Several chemical
78 classes of CpAM, including phenylpropanamide (PPA), heteroaryldihydropyrimidine
79 (HAP), and sulfamoylbenzamide (SBA) have been identified and the first compounds
80 are in early clinical trials (3). PPA-derivative AT130 selectively prevents pgRNA
81 packaging resulting in empty capsids that are morphologically identical to wild-type
82 capsids (11). HAP-derivative Bay41-4109 accelerates and misdirects capsid
83 assembly *in vitro* (12) and depletes newly-synthesized core protein by reducing its
84 half-life in cell culture (13). HAP_R01 is a novel HAP-type CpAM (Fig.1A) that binds
85 to the core protein dimer-dimer interface and effectively inhibits HBV replication and
86 HBeAg biosynthesis in HBV-replicating hepatoma cells (14-16).

87 While studies have shown that CpAMs can inhibit cccDNA formation during *de novo*
88 HBV infection (17-19), further mechanism-of-action (MOA) studies are needed to
89 elucidate whether and how CpAMs target capsid of incoming virus particle and affect
90 early stages of HBV infection. Studying this, we found that HAP_R01 inhibits
91 cccDNA formation in primary human hepatocytes (PHH), HepaRG and sodium
92 taurocholate co-transporting polypeptide (NTCP)-reconstituted hepatoma cells
93 (HepG2-NTCP-K7) (9) with 10- to 30-fold reduced efficacy compared to its inhibitory
94 effect on the formation of new virions. Mechanistic analysis demonstrated that
95 HAP_R01 directly acts on preformed HBV capsids resulting in aberrant core protein

96 polymers that are depleted in infected cells. HAP_R01 was also able to target the
97 capsids from incoming virions and reduce HBV particle infectivity. Furthermore, we
98 showed an additive antiviral effect of HAP_R01 when combined with entry inhibitors.

99

100 **Results**

101 **HAP_R01 inhibits cccDNA formation**

102 To study the effect of HAP_R01 in HBV infection, we used a highly permissive
103 HepG2 cell clone expressing NTCP (HepG2-NTCP-K7) that is well-characterized in
104 terms of infection kinetics and cccDNA dynamics and supporting 1-9 copies of
105 cccDNA per cell₍₉₎. Since HAP_R01 has been reported to prevent capsid formation
106 (15), we focused on its effects on a preformed capsid. Considering that cccDNA
107 formation is a slow process requiring 3 days (9), HepG2-NTCP-K7 cells were either
108 pretreated (pre) with HAP_R01 or treated during (d0-3) or after (d3-8) cccDNA
109 establishment (Fig.1B). Interestingly, cccDNA levels were significantly reduced when
110 HAP_R01 was applied during the first three days when HBV infection was being
111 established (Fig.1B). At equal doses, Bay41-4109 and AT130 reduced cccDNA levels
112 to a lesser extent than HAP_R01 (Fig. S1). The inhibitory effect on cccDNA was
113 independent of the moi (multiplicity of infection) of HBV used (Fig. S2). In contrast,
114 neither pretreatment i.e. 48 h treatment before infection (pre) nor treatment after
115 cccDNA formation (d3-8) diminished cccDNA levels (Fig.1B).

116 HAP_R01 inhibited new HBV-DNA production at a half-maximal effective
117 concentration (EC_{50}) ranging from 26.8 to 43.5 nM depending on cell type (Fig.1C).
118 However, 10- to 30-fold higher concentrations were needed to inhibit cccDNA
119 formation (EC_{50} 345-918 nM) upon HBV infection of HepG2-NTCP-K7 cells, HepaRG

120 cells, and primary human hepatocytes (PHH) (Fig.1D). Without treatment, HBV-
121 infected HepaRG cells and PHH contained 0.3-0.6 and 0.5-1 cccDNA copies/cell,
122 respectively. HAP_R01 had no detectable cytotoxicity under the conditions examined
123 (Fig.S3).

124 To delineate the time period during which HAP_R01 inhibits cccDNA formation, we
125 performed additional time-of-addition experiments (Fig.1E). Southern blot analysis
126 showed that the most significant reduction in cccDNA and protein-free rcDNA was
127 achieved by continuous HAP_R01 treatment for 3 days (d0-3) and, to a lesser extent,
128 by co-administering HAP_R01 during (d0-1) or early after (d1-2) HBV infection
129 (Fig.1E). In contrast, HAP_R01 failed to reduce cccDNA levels after 2 days post
130 infection (p.i.) (Fig.1E; d2-3). Secretion of HBeAg as an indirect marker of
131 transcriptionally active intra-nuclear cccDNA (9) correlated with cccDNA levels
132 (Fig.S4). Overall, these results demonstrate that HAP_R01 not only blocks formation
133 of new virions but also inhibits the establishment of cccDNA formation and are
134 consistent with previous reports showing that selected CpAMs have dual effects on
135 the virus life cycle (17-19).

136

137 **HAP_R01 alters capsid structure and integrity**

138 Given that HAP_R01 only showed an effect on establishing cccDNA during the first
139 48 h p.i. (Fig.1E), the most likely target was the incoming HBV capsid. To investigate
140 whether HAP_R01 can destabilize preformed capsids, we treated purified
141 recombinant HBV capsids composed of C-terminally truncated core proteins (amino
142 acids 1-149) with HAP_R01 and investigated structural alterations by electron
143 microscopy. As shown in Fig. 2A, HAP_R01 transformed 35-nm capsids into irregular

144 core protein structures of >100 nm size, showing a direct effect of HAP_R01 on
145 capsids.

146 Since *E.coli*-expressed HBV capsids do not contain HBV genomes, biochemical and
147 structural properties differ from those of mature, infectious capsids that contain
148 rcDNA (20). Thus, we established a method to isolate and analyze mature capsids
149 from hepatoma cells constitutively expressing the large HBV envelope protein (L-
150 HBsAg)-deficient, but replication-competent HBV genomes (HepG2-NTCP-K7-
151 H1.3L⁻) that we have recently described (9), and accumulate intracellular capsids
152 (Fig.S5). Three distinct populations were observed by dot-blot analysis of cesium
153 chloride (CsCl) density gradient fractions (Fig.2B). Fractions 8-9 (density 1.34-1.37
154 g/ml) contained capsids and viral nucleic acids, whereas fractions 11-12 (density
155 1.25-1.28 g/ml) exclusively contained capsids. Low-density fractions 16-18 (density
156 1.12-1.17 g/ml) appeared to contain core protein aggregates, as we observed a
157 slower and diffuse migration pattern (Fig.S6). Analysis of HBV-DNA content by qPCR
158 showed that capsids in fractions 8-9 had packaged viral DNA (Fig.2B).

159 Native agarose gel electrophoresis confirmed the identity of two capsid populations:
160 HBV-DNA-containing capsids (fractions 8-9) and empty capsids devoid of viral
161 nucleic acids (fractions 11-12) (Fig.S6). No loss of HBV-DNA signal after DNase I
162 treatment in pooled fraction 8-9 confirmed that HBV-DNA resides within capsids
163 (data not shown). Southern blot of DNA isolated from fractions 8-9 showed that the
164 majority of capsids contain either rcDNA (67%) or double-stranded linear (dl) DNA
165 (16%) (Fig.2C).

166 Having isolated mature capsids, we investigated if HAP_R01 would induce structural
167 changes of the capsids that can be detected by a mobility shift in native agarose gel

168 electrophoresis (21). Interestingly, we observed a mobility shift of capsid and HBV-
169 DNA bands already after 1 h HAP_R01 treatment (5000 nM) (Fig.2D; top),
170 suggesting an altered surface charge and shape of the capsid resulting in reduced
171 electrophoretic mobility. Capsid mobility was not altered in ETV-, Bay41-4109-, or
172 AT130-treated samples (Fig.2E; top). A similar mobility shift was observed when
173 empty capsids were incubated with HAP_R01, confirming HAP_R01-mediated
174 capsid distortion independent of packaged viral genomes (Fig.S7). Prolonged
175 incubation with HAP_R01 resulted in altered capsid mobility at 500 nM and, to a
176 lesser extent, at 50 nM and with Bay41-4109 at 5000 nM (Fig.2D-E; bottom).
177 Unexpectedly, we noted an increased capsid and HBV-DNA signal on the blot. This
178 likely resulted from an increased accessibility of the altered capsids for antibody and
179 probe binding, as the same pattern was observed using another anti-core antibody
180 (Fig.S8). These findings indicate that HAP_R01 can directly target HBV capsids and
181 induce abnormal core-protein structures more efficiently than other CpAMs including
182 Bay41-4109 and AT130.

183 To further our understanding of HAP_R01-induced structural alterations, we
184 analyzed the sensitivity of mature capsids to proteinase K alone or in combination
185 with DNase I after HAP_R01 treatment (Fig.2F). Proteinase K resulted in an
186 enhanced mobility shift of capsid and a reduced intensity of HBV-DNA bands (Fig.2F;
187 lanes 6-8), whereas additional DNase I treatment did not affect electrophoretic
188 mobility (Fig.2F; lanes 10-12). Besides the main capsid population, a population of
189 slow-migrating capsids (denoted with an asterisk) was detected in HAP_R01 treated
190 cells that apparently did not contain HBV-DNA anymore (Fig.2F; lanes 6-8 and 10-
191 12). In summary, our *in vitro* studies using both rcDNA-containing mature capsids
192 and *E.coli*-expressed capsids demonstrate that HAP_R01 can target, destabilize and

193 distort capsids resulting in aberrant core-protein polymers.

194

195 **HAP_R01 destabilizes and diminishes incoming capsids during *de novo* HBV**
196 **infection**

197 The results shown above suggested that HAP_R01 can target incoming capsids
198 during infection and inhibit cccDNA establishment. To determine optimal conditions
199 for the analysis of incoming capsids using the new method we have established, we
200 performed a time course study after infection with highly purified virions (Fig.3A). By
201 treating cells with trypsin and subsequent NP-40 lysis, we were able to analyze the
202 incoming, cytoplasmic capsids after virus uptake. Intracellular capsids, capsid-
203 associated HBV-DNA and core protein were detected starting from 1 h p.i. (Fig.3B-C).
204 Notably, a smear of both core protein and HBV-DNA migrating slower than capsids
205 and capsid-associated DNA was detected (denoted with asterisks) (Fig.3B). This
206 smear was not shown in newly-synthesized capsids (Fig.S9) indicating a certain
207 heterogeneity of incoming capsids that does not reflect the HBV inoculum (data not
208 shown). Quantitative analysis showed an increase of capsids over time with a
209 maximum reached at 8 h p.i. (Fig.3D). A gradual decrease observed after 8 h could
210 be explained by either capsid dissociation after HBV genome release into the
211 nucleus (22) or capsid degradation, exceeding the amount of newly entering virions.

212 At 5 h p.i. when most capsids entered the cells but the decay had not started yet,
213 HAP_R01 induced a 50% reduction in cytoplasmic capsids along with a modest
214 retardation in capsid electrophoretic mobility (Fig.3E). In contrast, ETV had no effect
215 on capsid levels or their mobility. Notably, a corresponding reduction in core protein
216 levels was observed by Western blot analysis (Fig.S10), suggesting HAP_R01-

- Ko et al.: HBV capsid modulators prevent infection -

217 mediated capsid depletion and degradation. Comparable results were observed
218 when measuring levels of capsid and core protein in an independent time course
219 experiment (Fig.3F). Treating cell lysates with proteinase K enhanced the
220 electrophoretic mobility shift of incoming capsids in particular after HAP_R01
221 treatment, while DNase had no additional effect (Fig.3E). This strongly suggests that
222 HAP_R01 deforms the incoming capsids, but structurally altered capsids still hold
223 HBV-DNA. To test a possibility that large, aberrant core polymers or a trace amount
224 of HBV-DNA released into the cytoplasm contribute to the reduced cccDNA formation
225 upon HAP_R01 treatment, we examined the expression of interferon-stimulated
226 genes (ISGs) at early time points after HBV infection (Fig.S11). HAP_R01 treatment
227 during HBV inoculation for 6 and 24 h did not induce ISG expression suggesting a
228 negligible role of host innate immune response. Overall, our data indicate that
229 HAP_R01 destabilizes the incoming capsid and thereby affects cccDNA
230 establishment during *de novo* infection.

231

232 **HAP_R01 targets extracellular HBV particles and reduces particle infectivity**

233 Since HAP_R01 showed the most significant reduction in cccDNA formation when
234 present during and up to 24 h after infection (Fig.1E), we wondered whether
235 HAP_R01 may target newly infecting particles. To investigate this, HBV particles
236 were incubated with HAP_R01 or other CpAMs and recovered by centrifugal filtration
237 prior to evaluating infectivity (Fig.4A). Treating HBV with HAP_R01 for 8 h or longer
238 resulted in a viral inoculum that established reduced levels of cccDNA (Fig.4B),
239 whereas preincubation with AT130 had no effect (Fig.4C). Bay41-4109 preincubation
240 also reduced HBV infectivity, although to a lower extent than HAP_R01. Of note,

- Ko et al.: HBV capsid modulators prevent infection -

241 HAP_R01 reduced the level of incoming capsid and core protein both during HBV
242 infection when HAP_R01 was in direct contact with HBV particles and shortly after
243 HBV infection when a direct contact of HAP_R01 with the inoculum was unlikely
244 (Fig.S12). Collectively, these results highlight a role for HAP_R01 to target both
245 extracellular HBV particles and intracellular, incoming capsids.

246

247 **HAP_R01 and entry inhibitors show additive effects on cccDNA establishment**

248 Given that HAP_R01 can prevent *de novo* cccDNA formation by altering incoming
249 capsid integrity and reducing HBV infectivity, we wondered if a combination of
250 HAP_R01 with entry inhibitors or a NUC could inhibit cccDNA formation more
251 efficiently. This would allow us to provide a rationale of potential application of
252 CpAMs in a combination with other antiviral agents. To evaluate this, HAP_R01 was
253 applied either alone or in combination with suboptimal doses of clinical-grade anti-
254 HBV immunoglobulin (HBIG, Hepatect CP™), the synthetic peptide myrcludex B
255 (MyrB) derived from preS1 domain of L-HBsAg (23), or ETV. HAP_R01 inhibited
256 cccDNA formation by >75% (Fig.5A). Combinatorial treatment with HBIG or MyrB
257 diminished cccDNA, HBeAg and HBsAg levels by >90% (Fig.5A). As expected, ETV
258 had no additive effect on cccDNA establishment implicating that the reverse
259 transcriptase activity of HBV polymerase is not required for the conversion of rcDNA
260 to cccDNA (24).

261 To model a “post-exposure” use of HAP_R01, we added HAP_R01 after HBV
262 infection and evaluated its antiviral activity. HAP_R01 reduced cccDNA, total
263 intracellular HBV-DNA, and HBeAg levels when added 12 h p.i. for 60 h, whereas

- Ko et al.: HBV capsid modulators prevent infection -

264 HBIG and MyrB did not have a significant antiviral effect (Fig.5B). Similar to the
265 treatment during infection, an additive effect on cccDNA formation was observed
266 when cells were treated with HBIG or MyrB during HBV inoculation but HAP_R01
267 was only added after HBV infection (Fig.5C). These data indicate that HAP_R01
268 exerts anti-HBV activity via a distinct MOA in comparison to entry inhibitors and has
269 the potential to prevent *de novo* cccDNA formation post-exposure.

270

271 Discussion

272 It is well known that CpAMs efficiently inhibit HBV reproduction by modulating the
273 assembly of newly forming capsids at a late step in the virus life cycle. However,
274 their effects on early stages of HBV infection i.e. before cccDNA formation are less
275 well characterized. In this study, we showed for the first time that HAP analogue
276 HAP_R01 physically alters capsid integrity in intact virions and early after HBV
277 infection. It is thus able to affect HBV infectivity and to inhibit cccDNA formation
278 during *de novo* HBV infection. This MOA was distinct from that of known entry
279 inhibitors allowing an additive antiviral activity during and shortly after HBV infection.

280 Several lines of evidence supported our finding. Firstly, HAP_R01 treatment during
281 establishment of infection significantly reduced cccDNA levels in HepG2-NTCP-K7
282 cells, in PHH and in HepaRG cells, however, at a concentration that was 10- to 30-
283 fold higher than the EC₅₀ needed to inhibit HBV replication. This is most likely
284 attributed to a reduced accessibility of HAP_R01 to assembled capsids compared to
285 core dimers that form new capsids (15). Our preliminary data showing that HAP_R01
286 preferentially binds to newly-translated core proteins rather than pre-existing core
287 proteins support our rationale (Ko et al., unpublished results). Secondly, neither

- Ko et al.: HBV capsid modulators prevent infection -

288 pretreatment of cells before HBV infection for 48 h nor HAP_R01 treatment after
289 cccDNA establishment affected cccDNA levels, indicating a targeting of mature HBV
290 capsids rather than a direct effect on cccDNA. Thirdly, HAP-type CpAMs HAP_R01
291 and Bay41-4109 and PPA-type AT130, but not the reverse transcriptase inhibitor
292 ETV, inhibited cccDNA formation indicating an antiviral activity of CpAMs during early
293 infection events. Fourthly, HAP_R01 was able to change the structure and physical
294 properties of preformed capsids resulting in an electrophoretic mobility shift and
295 increased sensitivity to proteinase K treatment. Lastly, HAP_R01 applied after
296 treatment with entry inhibitors HBIG or MyrB resulted in a further reduction of
297 cccDNA indicating that HAP_R01 prevents establishment of HBV infection via a
298 unique MOA in comparison to other entry inhibitors.

299 Our results are in line with recently published reports showing that selected CpAMs
300 can prevent cccDNA synthesis (17-19). *Berke et al.* first reported that JNJ-632 had
301 an effect on cccDNA formation when applied during or up to 8 h p.i. in PHH; however,
302 they could not dissect the underlying mechanism (17). *Guo et al.* reported that
303 Bay41-4109, ENAN-34017, and GLS4 inhibit cccDNA formation and provided
304 evidence that those CpAMs can act on preformed capsids (18). Although we could
305 confirm this effect, we did not observe contradicting effects as a consequence of
306 CpAM action i.e. inhibiting cccDNA synthesis during *de novo* infection vs. enhancing
307 cccDNA synthesis from intracellular amplification pathways.

308 In this study, we provide direct evidence that HAP_R01 can target “preformed”
309 capsids and change their physical properties by electron microscopic and
310 biochemical studies. Importantly, the effects of HAP_R01 on preformed capsids were
311 confirmed upon *de novo* infected cells. We first treated *E.coli*-expressed capsids,
312 purified after disassembly and reassembly to remove any non-assembled core

- Ko et al.: HBV capsid modulators prevent infection -

313 dimers, with HAP_R01. This resulted in aberrant core protein polymers, consistent
314 with observations that HAP compounds (Bay41-4109 and a fluorophore-labeled HAP)
315 can disrupt pre-assembled capsids *in vitro* (12, 25). To further investigate the effect
316 of HAP_R01 on mature, HBV-DNA containing capsids, we performed native agarose
317 gel electrophoresis. Electron microscopy was not possible due to low yield and purity
318 of mature capsids (data not shown). In native agarose gel electrophoresis, the
319 mobility of viral capsids is primarily determined by surface charge and mass, and
320 mobility shifts can be considered as an indicator of physical or structural changes
321 (21). We found a time- and concentration-dependent mobility shift of mature capsids
322 under HAP_R01 treatment. Bay41-4109, another HAP-type CpAM, induced mobility
323 shifts to a lesser degree, whereas AT130, a PPA-derivate CpAM, did not. This could
324 either reflect differences in MOA of the distinct chemical classes or biological EC₅₀
325 value.

326 Notably, HAP_R01-induced capsid alteration was confirmed in the HepG2-NTCP
327 HBV infection model that allows detection of incoming capsids. The addition of
328 HAP_R01 during HBV inoculation affected capsids released from purified virions
329 after virus entry and altered their electrophoretic mobility. Trypsin treatment ensured
330 that intracellular capsid and corresponding core protein were affected. Interestingly,
331 we found a reduction of the amount of core protein shortly after infection upon
332 HAP_R01 treatment that may be explained by accelerated proteasome-mediated
333 degradation of core protein (13). However, we did not detect an induction of ISGs
334 expression although activation of pattern recognition receptors by aberrant protein
335 structures or by rcDNA released from capsids within the cytoplasm would be
336 possible. This suggests that innate immune responses did not contribute to
337 HAP_R01-mediated capsid degradation. A weak functional DNA-sensing pathway in

338 hepatocytes (26) and the detection of HBV-DNA within the structurally altered
339 capsids would prevent the activation of cell-intrinsic immunity.

340 Although all our experiments point at a structural alteration of the incoming HBV
341 capsid upon HAP_R01 treatment, the question remains of why these structural
342 changes result in reduced cccDNA levels. Based on dynamics of HBV capsid that
343 could transiently dissociate and re-associate resulting from weak inter-subunit
344 interaction and alterations of tensional integrity due to HAP binding (27, 28) and the
345 degree of structural alteration of capsids, we envision two potential mechanisms that
346 are not mutually exclusive. Firstly, incoming capsids could be degraded if the
347 association of capsids and HAP_R01 is strong enough to induce severe structural
348 changes. This option is supported by the reduced core protein levels stemming from
349 incoming capsids. Secondly, altered capsids may have an impaired binding to host
350 factors resulting in defects in intracellular trafficking or nuclear import. Premature
351 disassembly of capsids or a wrong timing of viral genome release into the cytoplasm
352 instead of nuclear targeting may account for a reduced cccDNA establishment, as
353 proposed by *Guo et al.*(18). However, this seems unlikely in our experiments
354 because the majority of HBV-DNA was still located in structurally altered capsids and
355 resistant to DNase I treatment. The reason for this discrepancy is not clear at
356 present, but we speculate that this may be attributable to the source or isolation
357 methods of mature capsids or DNase treatment condition.

358 Interestingly, preincubation of HBV particles in the virus inoculum with HAP_R01
359 could also suppress the establishment of cccDNA in infected cells. This suggests
360 that HAP_R01 targeted the capsid within HBV virions and affected their infectivity. As
361 the viral envelope is composed of a cell-derived lipid bilayer with embedded viral
362 envelope proteins, it seems plausible that a small molecule possessing cell

363 membrane permeability could pass through a viral envelope. Of note, all antiviral
364 effects of HAP_R01 were obtained by simple addition of HAP_R01 into cell-culture
365 media indicating adequate cell permeability of HAP_R01. Additionally, HAP_R01 was
366 shown to be a moderately permeable compound in a parallel artificial membrane
367 permeability assay (PAMPA) and a Caco-2 permeability assay (data not shown). Our
368 finding suggests that HAP_R01 may not only be able to enter cells but even enter
369 into circulating infectious HBV particles in patient serum and alter their capsid
370 structure.

371 Supporting a distinct MOA of HAP_R01 on cccDNA establishment, we showed an
372 additive effect when HAP_R01 was combined with HBV entry inhibitors HBIG or
373 MyrB. Hereby, HAP_R01 was the only drug still having an effect 12 h post exposure,
374 i.e. after initial virus binding and uptake. A clinical situation where this maybe
375 interesting is mother-to-child transmission. However, this may be limited by the dose
376 required. A relatively high EC_{50} (345-918 nM) was determined to target incoming
377 capsids and inhibit cccDNA formation, and a dose achieving this effect *in utero* or
378 directly after birth may not be realistic. In chronic hepatitis B patients, the effect of
379 HAP_R01 on cccDNA formation effect will overlap with the inhibitory activity on
380 progeny virus production and thus may not become visible. Since EC_{50} alone is not
381 predictive for the clinical outcome of anti-HIV drugs (29), further assessment of
382 HAP_R01's performance (e.g., efficacy, toxicity, and bioavailability) in animal models
383 supporting the full HBV life cycle and, more importantly, in clinical trials will be
384 required to predict its superiority to other treatments and the role of HAP-resistant
385 HBV variants.

386 In summary, we deciphered the antiviral effects of a novel HAP derivative HAP_R01
387 possessing potent and core protein-specific anti-HBV activity. Our data highlight a

388 dual effect of HAP_R01 on cccDNA formation by targeting incoming virions and
389 capsids as well as on virion production by modulating capsid assembly, and support
390 further evaluation of a clinical benefit of HAP_R01.

391

392 **Materials and Methods**

393 **HBV infection**

394 HBV (genotype D; subtype ayw) was purified from the extracellular media of
395 HepAD38 cells by heparin affinity chromatography and a subsequent sucrose
396 gradient ultracentrifugation step and used as inoculum for infecting HepG2-NTCP-K7
397 cells as described (30, 31). HepG2-NTCP-K7 cells were seeded on collagen-coated
398 plates (e.g., 1×10^6 cells for 6-well plate and 2.5×10^5 cells for 24-well plate), pre-
399 differentiated with 2.5% DMSO for 2 days and infected with HBV in the presence of 4%
400 PEG6000 for at least 16 h.

401 **Quantitative real time PCR (qPCR) of HBV genomes**

402 cccDNA and total intracellular HBV-DNA were analyzed after extraction of total
403 cellular DNA using NucleoSpin Tissue kit (Macherey Nagel). DNA isolated from
404 HepG2-NTCP cells was treated with T5 exonuclease (NEB) for 30 min in 10 μ
405 reaction volume followed by heat-inactivation at 95°C for 5 min to remove non-
406 cccDNA species (9), while DNA isolated from HepaRG cells or PHH was directly
407 used for selective cccDNA detection as described (32). Target genes were
408 normalized by two reference genes encoding prion protein (*PRNP*) and
409 mitochondrial cytochrome c oxidase subunit 3 (*MT-CO3*) (9). DNA extracted from
410 extracellular media was used for qPCR to measure extracellular HBV-DNA contents.

411 **Southern blot analysis of cccDNA**

412 Protein-free, low-molecular-weight DNA species, including cccDNA, were extracted
413 using a modified Hirt procedure (9, 33). HBV-infected cells in a 35-mm dish were
414 lysed in 1 ml lysis buffer (50 mM Tris-HCl [pH7.5], 150 mM NaCl, 10 mM EDTA, and
415 1% SDS) with gentle agitation at 37°C for 1 h. KCl was added to 500 mM and the
416 lysate was incubated at 4°C overnight. After centrifugation, the supernatant was
417 subjected to phenol/chloroform extraction twice. Hirt DNA was precipitated using
418 isopropanol with 20 µg glycogen and subjected to Southern blot analysis with a
419 digoxigenin-labeled HBV-specific probe (30).

420 **Isolation and analysis of HBV capsids from hepatoma cells**

421 HepG2-NTCP-K7-H1.3L⁻ cells were lysed with 50 mM Tris-HCl [pH 8.0], 150 mM
422 NaCl, 1 mM EDTA, and 1% NP-40. Obtained cell lysate was layered on top of
423 preformed CsCl step-gradient in PBS (densities ranging 1.10-1.88 g/ml; 6 steps) and
424 centrifuged at 32,000 rpm for 16 h at 10°C in a Beckman SW32Ti rotor. Twenty-three
425 fractions (1.5 ml each) were collected. For capsid analysis, gradient fractions 8-9 and
426 11-12 were pooled, washed with 10 mM Tris-HCl [pH7.5]/150 mM NaCl/1 mM EDTA
427 and concentrated using a centrifugal filter device (100,000 MWCO). Capsids (ca. 1-5
428 ng) were resolved by a 1.2% agarose gel, transferred onto a PVDF membrane, and
429 visualized using anti-HBV core antibody (DAKO) (34). To analyze HBV-DNA within
430 capsids, the membrane was incubated with denaturation buffer (0.5 N NaOH/1.5 M
431 NaCl) for 1 min and 5 min with neutralization buffer (500 mM Tris-HCl [pH 7.0]/1.5 M
432 NaCl). After UV-crosslinking, HBV-DNA was visualized by hybridization with a
433 digoxigenin-labeled HBV-specific probe. For incoming capsids detection, 1-2x10⁶
434 cells were treated with trypsin-EDTA for 3 min to remove cell surface-bound but not

- Ko et al.: HBV capsid modulators prevent infection -

435 internalized HBV particles, lysed in 100 μ l 1% NP-40 buffer for 15 min on ice and
436 centrifuged to pellet debris and nuclei. The obtained cell lysate was directly used for
437 capsid analysis.

438 **Transmission electron microscopy**

439 Purified *E.coli*-expressed HBV capsids, described in the Supplementary Methods,
440 were absorbed onto glow-discharged carbon-coated grids. The grids were then
441 stained with 1% [w/v] uranyl acetate for 10 sec, washed with deionized water, and
442 dried for 20 min. Images were acquired under a FEI-120kV transmission electron
443 microscope with a magnification of 67,000x.

444

445 **Acknowledgements**

446 We thank Stephan Urban for providing Myrcludex B and Jochen M. Wettengel, Jan-
447 Hendrick Bockmann, and Daniela Stadler for their helpful advice. We thank Jane A.
448 McKeating for critical reading of the manuscript.

449

450 **Financial support**

451 The study was supported by the German Research Foundation (DFG) via TRR 179
452 (project TP14) and by the German Center for Infection Research (DZIF, projects
453 05.806 and 05.707) to UP and by the Roche Postdoc Fellowship Program to CK.

454

455 **Conflict of interest**

- Ko et al.: HBV capsid modulators prevent infection -

456 XZ, ZX and LG are employees of Roche R&D Center (China) Ltd. UP serves as ad
457 hoc advisor for Arbutus, Vir Biotechnology, Vaccitech, Gilead, Merck, Roche and J&J.

458

459 **Author contributions**

460 CK, LG, UP initiated and designed the study; CK, RB, XZ, ZX, CB, JS performed the
461 experiments; FWRV provided key materials and contributed to the execution of the
462 experiments; CK, UP wrote the manuscript.

463

464 **References**

- 465 1. WHO. 2019. Hepatitis B, Fact sheet. [https://www.who.int/news-room/fact-](https://www.who.int/news-room/fact-sheets/detail/hepatitis-b)
466 [sheets/detail/hepatitis-b](https://www.who.int/news-room/fact-sheets/detail/hepatitis-b). Accessed Updated 18 July 2019.
- 467 2. Schweitzer A, Horn J, Mikolajczyk RT, Krause G, Ott JJ. 2015. Estimations of worldwide
468 prevalence of chronic hepatitis B virus infection: a systematic review of data published
469 between 1965 and 2013. *Lancet* 386:1546-55.
- 470 3. Lok AS, Zoulim F, Dusheiko G, Ghany MG. 2017. Hepatitis B cure: From discovery to
471 regulatory approval. *J Hepatol* 67:847-861.
- 472 4. Seeger C, Mason WS. 2015. Molecular biology of hepatitis B virus infection. *Virology* 479-
473 480C:672-686.
- 474 5. Hong X, Kim ES, Guo H. 2017. Epigenetic regulation of hepatitis B virus covalently closed
475 circular DNA: Implications for epigenetic therapy against chronic hepatitis B. *Hepatology*
476 66:2066-2077.
- 477 6. Lewellyn EB, Loeb DD. 2011. The arginine clusters of the carboxy-terminal domain of the
478 core protein of hepatitis B virus make pleiotropic contributions to genome replication. *J*
479 *Virol* 85:1298-309.
- 480 7. Tan Z, Pionek K, Unchwaniwala N, Maguire ML, Loeb DD, Zlotnick A. 2015. The interface
481 between hepatitis B virus capsid proteins affects self-assembly, pregenomic RNA
482 packaging, and reverse transcription. *J Virol* 89:3275-84.
- 483 8. Chu TH, Liou AT, Su PY, Wu HN, Shih C. 2014. Nucleic acid chaperone activity associated
484 with the arginine-rich domain of human hepatitis B virus core protein. *J Virol* 88:2530-43.
- 485 9. Ko C, Chakraborty A, Chou WM, Hasreiter J, Wettengel JM, Stadler D, Bester R, Asen T,
486 Zhang K, Wisskirchen K, McKeating JA, Ryu WS, Protzer U. 2018. Hepatitis B virus genome

- 487 recycling and de novo secondary infection events maintain stable cccDNA levels. *J Hepatol*
488 69:1231-1241.
- 489 10. Zlotnick A, Venkatakrishnan B, Tan Z, Lewellyn E, Turner W, Francis S. 2015. Core protein: A
490 pleiotropic keystone in the HBV lifecycle. *Antiviral Res* 121:82-93.
- 491 11. Feld JJ, Colledge D, Sozzi V, Edwards R, Littlejohn M, Locarnini SA. 2007. The
492 phenylpropenamide derivative AT-130 blocks HBV replication at the level of viral RNA
493 packaging. *Antiviral Res* 76:168-77.
- 494 12. Stray SJ, Zlotnick A. 2006. BAY 41-4109 has multiple effects on Hepatitis B virus capsid
495 assembly. *J Mol Recognit* 19:542-8.
- 496 13. Deres K, Schroder CH, Paessens A, Goldmann S, Hacker HJ, Weber O, Kramer T, Niewohner
497 U, Pleiss U, Stoltefuss J, Graef E, Koletzki D, Masantschek RN, Reimann A, Jaeger R, Gross R,
498 Beckermann B, Schlemmer KH, Haebich D, Rubsamen-Waigmann H. 2003. Inhibition of
499 hepatitis B virus replication by drug-induced depletion of nucleocapsids. *Science* 299:893-
500 6.
- 501 14. Qiu Z, Lin X, Zhang W, Zhou M, Guo L, Kocer B, Wu G, Zhang Z, Liu H, Shi H, Kou B, Hu T,
502 Hu Y, Huang M, Yan SF, Xu Z, Zhou Z, Qin N, Wang YF, Ren S, Qiu H, Zhang Y, Zhang Y,
503 Wu X, Sun K, Zhong S, Xie J, Ottaviani G, Zhou Y, Zhu L, Tian X, Shi L, Shen F, Mao Y, Zhou
504 X, Gao L, Young JAT, Wu JZ, Yang G, Mayweg AV, Shen HC, Tang G, Zhu W. 2017.
505 Discovery and Pre-Clinical Characterization of Third-Generation 4-H
506 Heteroaryldihydropyrimidine (HAP) Analogues as Hepatitis B Virus (HBV) Capsid Inhibitors.
507 *J Med Chem* 60:3352-3371.
- 508 15. Zhou Z, Hu T, Zhou X, Wildum S, Garcia-Alcalde F, Xu Z, Wu D, Mao Y, Tian X, Zhou Y,
509 Shen F, Zhang Z, Tang G, Najera I, Yang G, Shen HC, Young JA, Qin N. 2017.
510 Heteroaryldihydropyrimidine (HAP) and Sulfamoylbenzamide (SBA) Inhibit Hepatitis B Virus
511 Replication by Different Molecular Mechanisms. *Sci Rep* 7:42374.
- 512 16. Yan Z, Wu D, Hu H, Zeng J, Yu X, Xu Z, Zhou Z, Zhou X, Yang G, Young JAT, Gao L. 2019.
513 Direct Inhibition of Hepatitis B e Antigen by Core Protein Allosteric Modulator. *Hepatology*
514 70:11-24.
- 515 17. Berke JM, Dehertogh P, Vergauwen K, Van Damme E, Mostmans W, Vandyck K, Pauwels F.
516 2017. Capsid Assembly Modulators Have a Dual Mechanism of Action in Primary Human
517 Hepatocytes Infected with Hepatitis B Virus. *Antimicrob Agents Chemother* 61:e00560-17.
- 518 18. Guo F, Zhao Q, Sheraz M, Cheng J, Qi Y, Su Q, Cuconati A, Wei L, Du Y, Li W, Chang J, Guo
519 JT. 2017. HBV core protein allosteric modulators differentially alter cccDNA biosynthesis
520 from de novo infection and intracellular amplification pathways. *PLoS Pathog* 13:e1006658.
- 521 19. Lahlali T, Berke JM, Vergauwen K, Foca A, Vandyck K, Pauwels F, Zoulim F, Durantel D. 2018.
522 Novel Potent Capsid Assembly Modulators Regulate Multiple Steps of the Hepatitis B Virus
523 Life Cycle. *Antimicrob Agents Chemother* 62:e00835-18.
- 524 20. Cui X, Ludgate L, Ning X, Hu J. 2013. Maturation-associated destabilization of hepatitis B
525 virus nucleocapsid. *J Virol* 87:11494-503.
- 526 21. Wu S, Luo Y, Viswanathan U, Kulp J, Cheng J, Hu Z, Xu Q, Zhou Y, Gong GZ, Chang J, Li Y,

- 527 Guo JT. 2018. CpAMs induce assembly of HBV capsids with altered electrophoresis
528 mobility: Implications for mechanism of inhibiting pgRNA packaging. *Antiviral Res* 159:1-
529 12.
- 530 22. Rabe B, Delaleau M, Bischof A, Foss M, Sominskaya I, Pumpens P, Cazenave C, Castroviejo
531 M, Kann M. 2009. Nuclear entry of hepatitis B virus capsids involves disintegration to
532 protein dimers followed by nuclear reassociation to capsids. *PLoS Pathog* 5:e1000563.
- 533 23. Petersen J, Dandri M, Mier W, Lutgehetmann M, Volz T, von Weizsacker F, Haberkorn U,
534 Fischer L, Pollok JM, Erbes B, Seitz S, Urban S. 2008. Prevention of hepatitis B virus
535 infection in vivo by entry inhibitors derived from the large envelope protein. *Nat*
536 *Biotechnol* 26:335-41.
- 537 24. Qi Y, Gao Z, Xu G, Peng B, Liu C, Yan H, Yao Q, Sun G, Liu Y, Tang D, Song Z, He W, Sun Y,
538 Guo JT, Li W. 2016. DNA Polymerase kappa Is a Key Cellular Factor for the Formation of
539 Covalently Closed Circular DNA of Hepatitis B Virus. *PLoS Pathog* 12:e1005893.
- 540 25. Schlicksup CJ, Wang JC, Francis S, Venkatakrisnan B, Turner WW, VanNieuwenhze M,
541 Zlotnick A. 2018. Hepatitis B virus core protein allosteric modulators can distort and
542 disrupt intact capsids. *Elife* 7:e31473.
- 543 26. Thomsen MK, Nandakumar R, Stadler D, Malo A, Valls RM, Wang F, Reinert LS, Dagnaes-
544 Hansen F, Hollensen AK, Mikkelsen JG, Protzer U, Paludan SR. 2016. Lack of immunological
545 DNA sensing in hepatocytes facilitates hepatitis B virus infection. *Hepatology* 64:746-59.
- 546 27. Hadden JA, Perilla JR. 2018. All-atom molecular dynamics of the HBV capsid reveals
547 insights into biological function and cryo-EM resolution limits. *Elife* 7:e32478.
- 548 28. Ceres P, Zlotnick A. 2002. Weak protein-protein interactions are sufficient to drive
549 assembly of hepatitis B virus capsids. *Biochemistry* 41:11525-31.
- 550 29. Shen L, Peterson S, Sedaghat AR, McMahon MA, Callender M, Zhang H, Zhou Y, Pitt E,
551 Anderson KS, Acosta EP, Siliciano RF. 2008. Dose-response curve slope sets class-specific
552 limits on inhibitory potential of anti-HIV drugs. *Nat Med* 14:762-6.
- 553 30. Burwitz BJ, Wettengel JM, Muck-Hausl MA, Ringelhan M, Ko C, Festag MM, Hammond KB,
554 Northrup M, Bimber BN, Jacob T, Reed JS, Norris R, Park B, Moller-Tank S, Esser K, Greene
555 JM, Wu HL, Abdulhaqq S, Webb G, Sutton WF, Klug A, Swanson T, Legasse AW, Vu TQ,
556 Asokan A, Haigwood NL, Protzer U, Sacha JB. 2017. Hepatocytic expression of human
557 sodium-taurocholate cotransporting polypeptide enables hepatitis B virus infection of
558 macaques. *Nat Commun* 8:2146.
- 559 31. Seitz S, Iancu C, Volz T, Mier W, Dandri M, Urban S, Bartenschlager R. 2016. A Slow
560 Maturation Process Renders Hepatitis B Virus Infectious. *Cell Host Microbe* 20:25-35.
- 561 32. Xia Y, Stadler D, Ko C, Protzer U. 2017. Analyses of HBV cccDNA Quantification and
562 Modification. *Methods Mol Biol* 1540:59-72.
- 563 33. Yan H, Zhong G, Xu G, He W, Jing Z, Gao Z, Huang Y, Qi Y, Peng B, Wang H, Fu L, Song M,
564 Chen P, Gao W, Ren B, Sun Y, Cai T, Feng X, Sui J, Li W. 2012. Sodium taurocholate
565 cotransporting polypeptide is a functional receptor for human hepatitis B and D virus. *Elife*
566 1:e00049.

- Ko et al.: HBV capsid modulators prevent infection -

- 567 34. Ko C, Lee S, Windisch MP, Ryu WS. 2014. DDX3 DEAD-Box RNA Helicase Is a Host Factor
568 That Restricts Hepatitis B Virus Replication at the Transcriptional Level. *J Virol* 88:13689-98.
569
570

571 **Figure legends**572 **Fig. 1. Evaluation of the effect of HAP_R01 on cccDNA establishment**

573 (A) Chemical structure of HAP_R01. (B) HepG2-NTCP-K7 cells were infected with
574 HBV at an moi of 100 vp/cell and treated with 5 μ M HAP_R01 at different time
575 periods as indicated. Extracted total cellular DNA was subjected to cccDNA qPCR.
576 (C,D) Cells were treated with increasing concentrations of HAP_R01 either from 3
577 dpi until 9 dpi (C) or at the time of HBV inoculation for 3 days (D). Levels of
578 intracellular HBV-DNA (C) and cccDNA (D) were analyzed by qPCR. The half
579 maximal effective concentration (EC_{50}) of HAP_R01 required to inhibit viral DNA
580 production and cccDNA formation was calculated by nonlinear regression analysis
581 after generating a dose response curve. (E) HepG2-NTCP-K7 cells were infected
582 with HBV at an moi of 500 vp/cell and treated with 5 μ M HAP_R01 at different time
583 periods as indicated. DNA extracted after the Hirt procedure was assayed by
584 Southern blot analysis with an HBV-DNA probe. cccDNA and protein-free rcDNA
585 (PF-rcDNA) are denoted. Restriction fragments of HBV-DNA (3.2 to 1.9 kb) serve as
586 a size marking ladder. A representative image is shown. cccDNA bands were
587 quantified from four independent experiments and Southern blots, and the
588 percentage values of cccDNA (relative to untreated control) were plotted in a bar
589 graph (mean \pm SD; n=4). Student's t test (**p \leq 0.001, *p \leq 0.05, ns: not significant). vp:
590 virus particle. moi: multiplicity of infection. dpi: day post-infection.

591

592 **Fig. 2. Effect of HAP_R01 on capsids *in vitro***

593 (A) Recombinant capsids purified from *E.coli* expressing C-terminally truncated form
594 of core protein (Cp1-149) were either mock-treated or treated with 20 μ M HAP_R01

- Ko et al.: HBV capsid modulators prevent infection -

595 for 3 h in 250 mM NaCl and 50 mM HEPES [pH7.4]. Electron microscopic images of
596 negatively stained capsids are shown. (B) Cytoplasmic lysate from HepG2-NTCP-
597 K7-H1.3L⁻ cells was subjected to CsCl density gradient ultracentrifugation and
598 twenty-three fractions were collected from bottom to top. Aliquots of each fraction
599 were transferred onto a PVDF membrane by using a dot-blot device, and capsid
600 levels were analyzed by immunoblotting with an anti-core antibody (DAKO) which
601 preferentially recognizes capsid rather than denature core protein (22). Viral nucleic
602 acids on the same membrane were subsequently detected by an HBV-DNA probe.
603 Additionally, total cellular DNA was extracted from each fraction and analyzed by
604 HBV-DNA qPCR. Relative amounts of capsid and total intracellular HBV-DNA in each
605 fraction were quantified and plotted together with CsCl densities. (C) DNA was
606 extracted from pooled fraction 8-9 and subjected to Southern blot analysis. rcDNA,
607 dlDNA, single-stranded (ss) DNA are denoted together with a 3.2-kb HBV-DNA
608 fragment serving as a size marker. (D-F) Capsid and capsid-associated HBV-DNA
609 contents were analyzed by native agarose gel analysis in the absence of SDS (see
610 Supplementary materials). The concentration of DMSO was 1% in all conditions.
611 Pooled fraction 8-9 was treated with either increasing concentrations of HAP_R01 (D)
612 or different anti-HBV compounds (5 μ M each) (E) at 37°C for 1 h and 6 h. (F) Pooled
613 fraction 8-9 was either mock-treated or treated with 5 μ M HAP_R01 at 37°C for 1 h.
614 Increasing concentrations of proteinase K alone or in combination with DNase I (5
615 units) were added for additional 1 h.

616

617 **Fig. 3. Effect of HAP_R01 on incoming capsids in *de novo* HBV infection**

618 (A) HBV-infected (500 vp/cell) HepG2-NTCP-K7 cells were harvested at different
619 time points. Before harvest, cells were treated with trypsin for 3 min to remove

620 membrane-associated input virus particles. Cytoplasmic capsid and capsid-
621 associated HBV-DNA (B) and core protein (C) were detected by native agarose gel
622 analysis and Western blot analysis, respectively. β -actin serves as a loading control.
623 (D) Relative amounts of capsid and HBV-DNA within the capsid, and core protein
624 were quantified and plotted with 8 h-HBV inoculation condition set to 100%. (E)
625 HepG2-NTCP-K7 cells were either treated with PEG (mock-infection) or infected with
626 HBV at an moi of 500 vp/cell for 5 h in the presence or absence of HAP_R01 or ETV
627 (5 μ M each). Obtained cytoplasmic lysate were either mock-treated or treated with
628 proteinase K (1 mg/ml) alone or proteinase K plus DNase I (5 units) at 37°C for 1 h.
629 Capsid and capsid-associated HBV-DNA were analyzed and quantified relative to
630 untreated control. (F) HepG2-NTCP-K7 cells were infected with HBV in the presence
631 or absence of HAP_R01. Cytoplasmic capsid and core protein levels were analyzed
632 at indicated time points. PEG: polyethylene glycol

633

634 **Fig. 4. Effect of CpAMs on the infectivity of HBV particles**

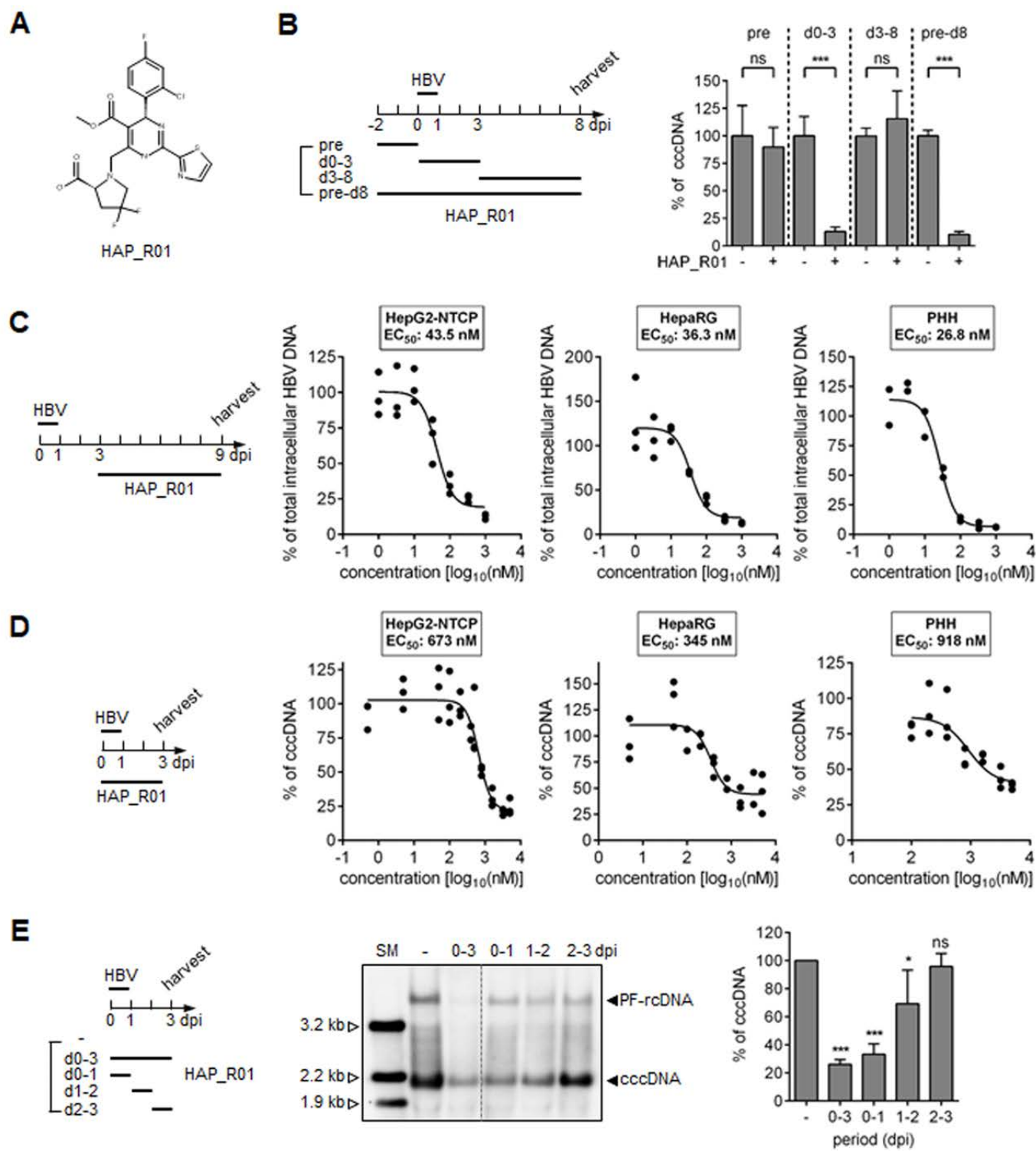
635 (A) An illustration showing a procedure of HAP_R01 preincubation with purified HBV
636 particles and recovery for following HBV infectivity test. HBV particles were
637 incubated with antivirals in a reaction volume of 1 ml of DMEM medium containing
638 penicillin/streptomycin. HBV particles were then recovered by using a Vivaspin
639 centrifugal concentrator (100,000 MWCO; Sartorius) during which an excess
640 amount of antivirals was washed away. (B) HBV particles were preincubated with
641 either DMSO or HAP_R01 (5 μ M) for increasing times at 37°C and recovered as
642 depicted in panel A. HepG2-NTCP-K7 cells were infected with DMSO- or HAP_R01-
643 preincubated HBV. cccDNA levels were analyzed by qPCR relative to control. (C)
644 HBV particles preincubated with indicated anti-HBV compounds (5 μ M each; 37°C

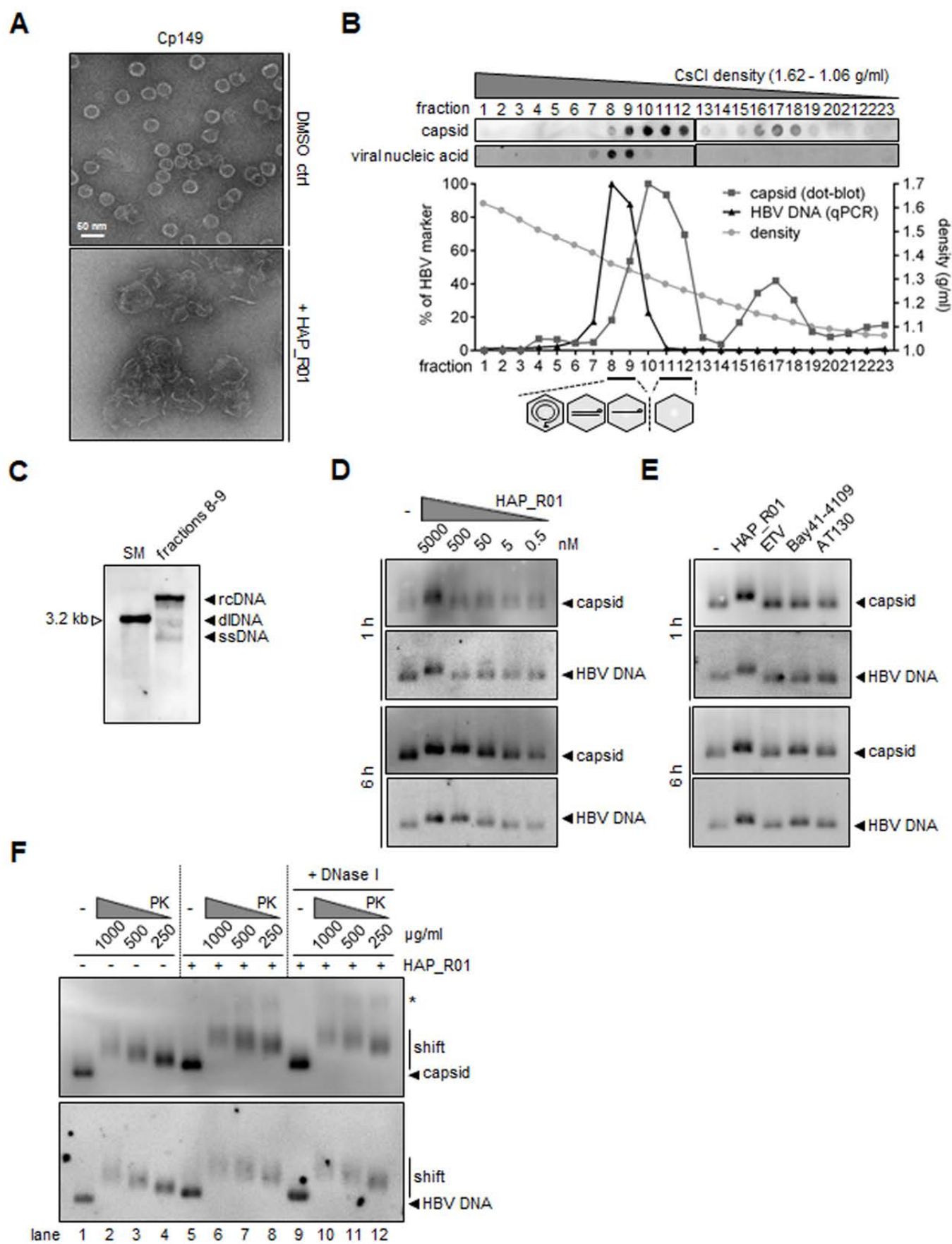
645 for 16 h) were used for HBV infection as similar to panel B. At 7 dpi, intracellular viral
646 DNA and extracellular HBeAg levels were determined by qPCR and ELISA,
647 respectively. Student's t test (***p ≤0.001, **p ≤0.01, *p ≤0.05, ns: not significant).

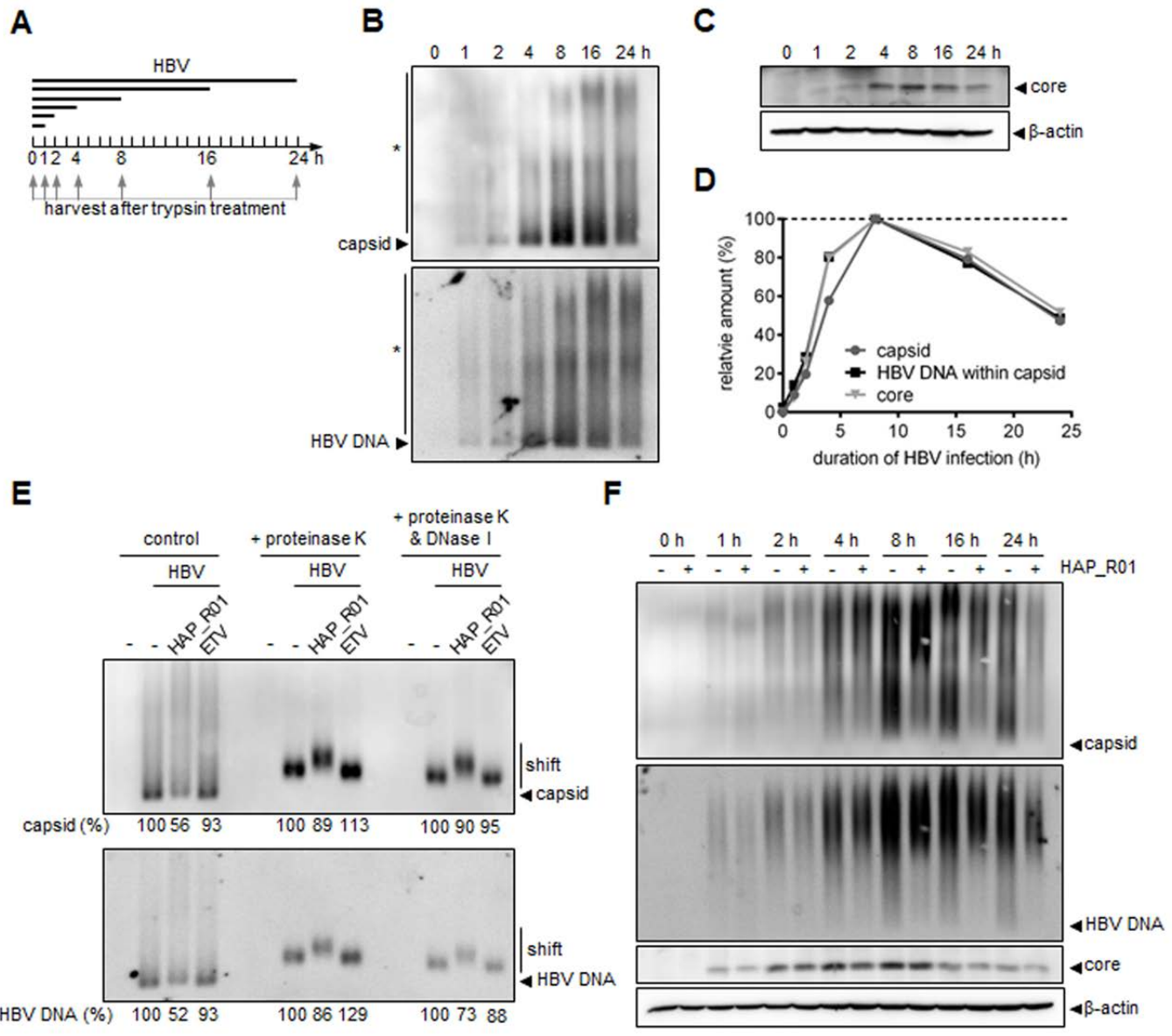
648

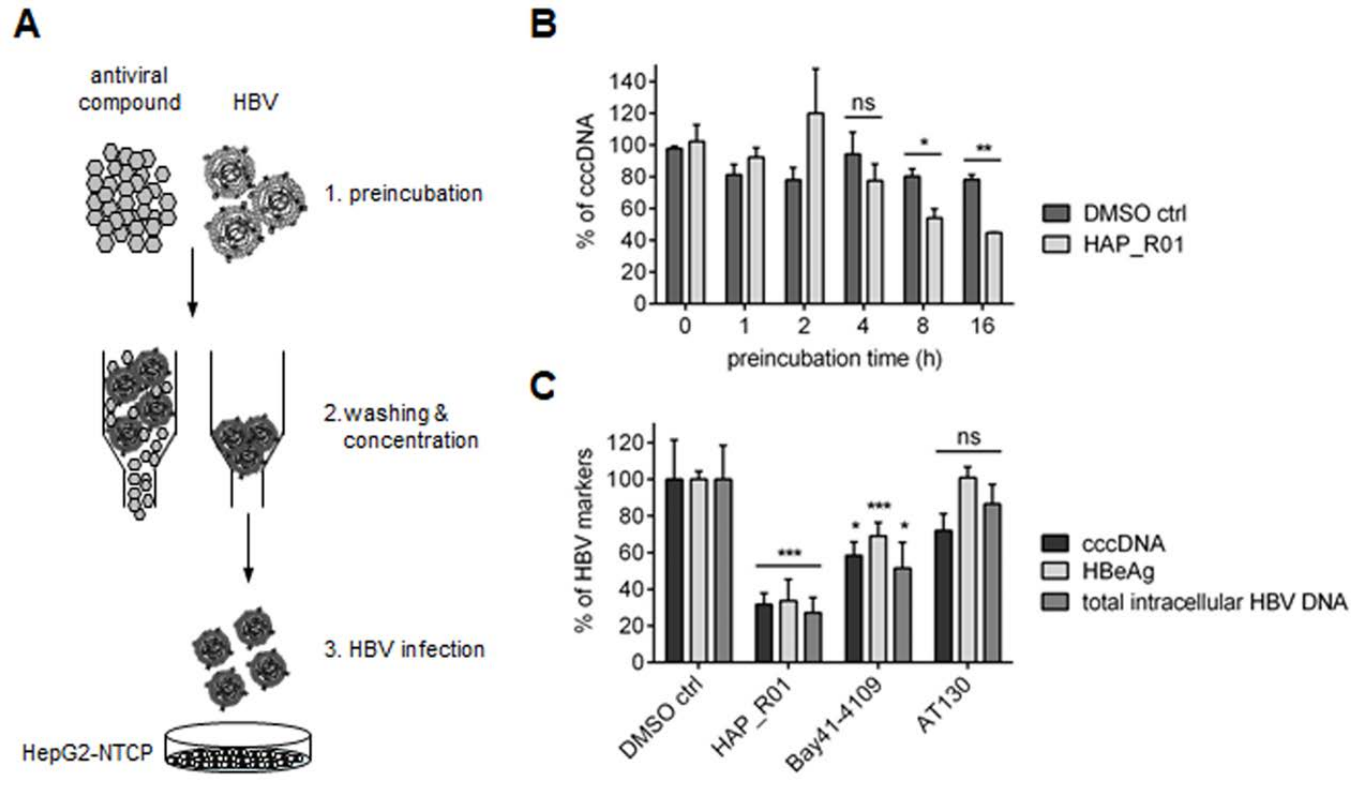
649 **Fig. 5. Evaluation of efficacy of HAP_R01 treatment in combination with entry**
650 **inhibitors on cccDNA formation**

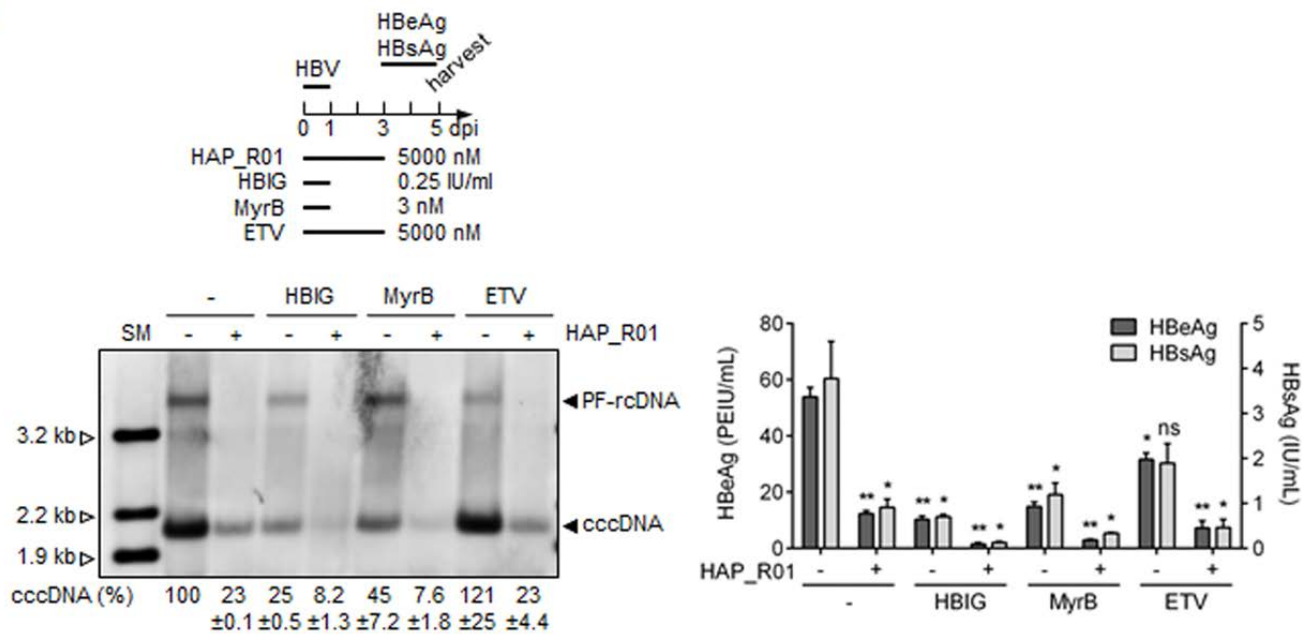
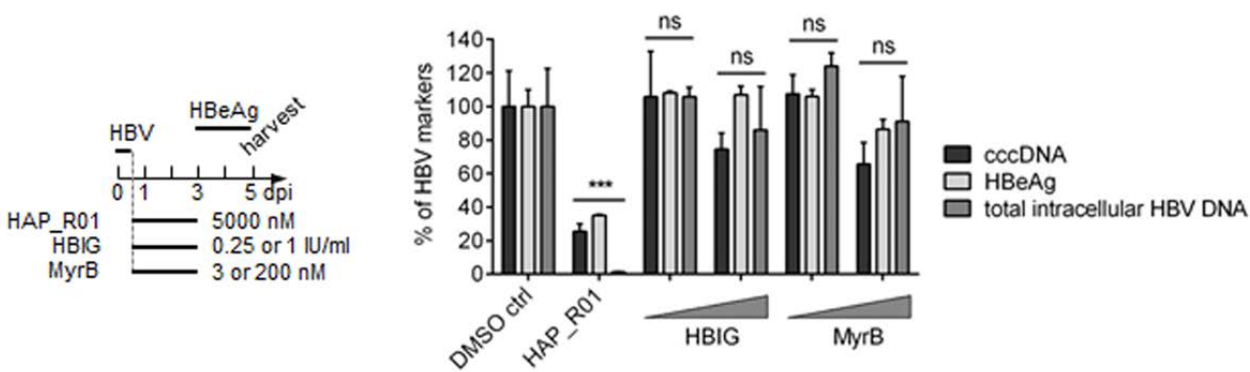
651 (A) HepG2-NTCP-K7 cells were infected with HBV at an moi of 500 vp/cell and
652 treated with different anti-HBV drugs for indicated time periods either alone or in
653 combination. At 5 dpi, cellular DNA extracted after Hirt method was subjected to
654 Southern blot analysis (left). cccDNA and PF-rcDNA are denoted. cccDNA bands
655 were quantified and shown as mean±SD from two independent experiments. Three
656 HBV-DNA fragments (3.2, 2.2, and 1.9 kb) serve as size markers. HBsAg and
657 HBeAg in extracellular media were quantified by immunoassay (right). (B,C) HepG2-
658 NTCP-K7 cells were infected with an moi of 100 vp/cell for 12 h. During or after HBV
659 inoculation, different anti-HBV drugs were applied either alone or in combination as
660 indicated. cccDNA, total intracellular HBV-DNA, and HBeAg levels were analyzed by
661 qPCR and ELISA. Student's t test (***p ≤0.001, **p ≤0.01, *p ≤0.05, ns: not
662 significant).









A**B****C**